

Preparation of an Electrochemical Sensor Based on Multi-Walled Carbon Nanotubes/Molecularly Imprinted Polymers for the Detection of Capsaicin in Gutter Oil by Differential Pulse Voltammetry

Mi Wang¹, Bin Gao², Yu Xing^{1,*}, Xingliang Xiong^{2,*}

¹ Department of forensic medicine, Chongqing Medical University, #1 Yixueyuan Road, Chongqing 400016, China.

² Laboratory of Biomedical Engineering, Chongqing Medical University, #1 Yixueyuan Road, Chongqing 400016, China.

*E-mail: 100485@cqmu.edu.cn, xxlsober@sina.com

Received: 13 May 2020 / Accepted: 4 July 2020 / Published: 10 August 2020

Despite great technological advancements, the rapid, on-the-spot identification of gutter oils continues to be a great challenge. In this study, capsaicin is chosen as a biochemical marker of gutter oil, and an electrochemical sensor of this marker is developed based on multi-walled carbon nanotubes/molecularly imprinted polymers (MWCNTs-MIP). The MIP-modification of MWCNTs is achieved using 4-vinylpyridine as a functional monomer and capsaicin as a template. The electrochemical behavior of the prepared sensor is evaluated by differential pulse voltammetry, and the optimal conditions are determined. The results show a significantly linear response of the sensor towards capsaicin in the range of 0.05×10^{-6} - 1×10^{-4} mol L⁻¹, with a limit of detection (LOD) of about 0.02 μmol L⁻¹. The sensor also exhibits excellent selectivity, repeatability, and stability in real sample detection.

Keywords electrochemical sensor, molecularly imprinted polymers, gutter oil, capsaicin

1. INTRODUCTION

Food safety is closely related to public health. As such, it has always been an issue of global concern. For example, gutter oil, a cooking oil commonly used in restaurants, is significantly harmful to the human body due to high contents of carcinogenic and toxic substances such as cholesterol, trans-fatty acids, heavy metals, condiments, dioxins, and bacteria. Nevertheless, used gutter oil is often refined and sold on the market as an edible oil [1, 2]. Consumers can usually rely on the distinctive properties of smell and color to identify gutter oils in the market (intuitionistic judgment method). However, advances in reprocessing technology have enabled the improvement of gutter oil color and smell such that it can no longer be distinguished from edible oil based on these properties [3]. Other methods of

gutter oil identification are based on the detection of marker compounds, such as acetic acid, 3-butene nitrile, zingiberene, anethole, allyl isothiocyanate, trans-fatty acids, triacylglycerols, cholesterol, antioxidants, and furan, in the oil residues [4-12]. Still, treatment processes, including neutralization, washing, drying, bleaching, filtering, and deodorizing can decrease the concentrations of these markers to very low levels, thereby impeding detection [13]. As such, highly sensitive analytical techniques, such as chromatography, chromatography coupled with mass spectrometry (MS), and magnetic resonance spectroscopy have been applied in the analysis of gutter oil [4-9]. Despite the advantages of these techniques, they cannot be used in field testing due to certain limitations, such as tedious sample processing, the need for professionals, and high detection costs. Therefore, the effective identification of gutter oil requires both a portable detection method and the selection of an appropriate marker.

Capsaicin (CAPS), one of the major active ingredients in hot pepper, is a component of gutter oil residues. Owing to its lipophilicity and high boiling point, capsaicin cannot be easily eliminated by oil refinement, and thus, it is a suitable marker for the identification of gutter oils [3]. Electrochemical techniques based on direct-electron-transfer-shuttle-free detection have long been used for the analysis of capsaicin [14]. Various kinds of electrodes, including multi-walled carbon nanotube modified basal plane pyrolytic graphite (MWCNT-BPPGE), multi-walled carbon nanotube screen-printed (MWCNT-SPE), and amino-functionalized mesoporous silica-modified carbon paste (NH₂-FMS/CPE) electrodes, have shown great efficiency in detecting this compound due to their remarkable sensitivity, repeatability, and stability [15, 16]. Unfortunately, the application of these electrodes is limited by low selectivity, high costs, and the complexity of the material reprocessing steps. The PAL enzyme/Nafion/MWCNTs/Pt-E electrode has excellent selectivity and good sensitivity towards capsaicin [17], but it is relatively unstable due to the degradation of the enzyme under particular conditions of temperature and pressure [14].

Molecularly imprinted polymers (MIPs), also referred to as synthetic antibodies, are widely used in the artificial recognition of template molecules. The recognition mechanism of these materials is similar to that of some natural biomolecular adsorption systems, such as the antibody/antigen, receptor/ligand, and enzyme/substrate systems, that can mimic biological receptors [18, 19]. Like these systems, MIPs possess specific analyte-binding abilities. Moreover, they are chemically and thermally stable, durable, and highly selective. Therefore, MIPs have great potential for use in electrochemical sensors.

In this work, molecularly imprinted polymers were synthesized over the surface of multi-walled carbon nanotubes using capsaicin as template and 4-vinylpyridine as monomer. The synthesized MWCNT-MIP was coated on a glassy carbon electrode (GCE) and used to determine capsaicin concentrations in gutter oil samples. The results demonstrate that the MWCNT-MIP-based electrode exhibits remarkable specificity and sensitivity, and thus, it can be applied in the identification of gutter oils.

2. EXPERIMENTAL

2.1. Apparatus and reagents

MWCNTs (internal diameter 3–5 nm, outer diameter 8–15 nm, length ~50 μm, and purity > 95%),

allylamine, p-aminophenol, 2,2-azoisobutyronitrile (AIBN), and CAPS were purchased from Sigma Aldrich (Shanghai, China). Commercial ethyleneglycol dimethacrylate (EGDMA) and 4-vinyl pyridine (4-VP) products were also bought from Sigma Aldrich, but they were distilled under reduced pressure to remove inhibitors before use. Thionyl chloride (SOCl_2), tetrahydrofuran (THF), dimethylformamide (DMF), and acetic acid (HAc) were obtained from Aldrich, and Britton-Robinson buffer solution was prepared with H_3PO_4 , HAc, and H_3BO_3 , purchased from Aldrich as well.

The electrochemical data was acquired using a three-electrode CHI660E workstation (ChenHua Instruments, Shanghai, China) comprised of an MWCNTs-NIP or MWCNTs-MIP GCE working electrode, a platinum counter electrode, and a saturated Ag/AgCl reference electrode. The surface morphology of the MIPs was analyzed by scanning electron microscopy (SEM), and functional group analysis was performed using Fourier transform infrared spectroscopy (FTIR). High performance liquid chromatography (HPLC) data was acquired using an Acquity UPLC system (Waters Corp Milford, MA, USA) equipped with a binary pump and a Xevo TQ MS mass spectrometer (Waters Corp). Chromatographic separation was achieved on an Acquity UPLC BEH C18 column ($100 \text{ mm} \times 2.1 \text{ mm} \times 1.8 \mu\text{m}$) using gradient elution. The injection volume and flow rate were set to $20 \mu\text{L}$ and 0.3 mL min^{-1} , respectively, and the mobile phase consisted of water:formic acid (100:0.1 v/v, solvent A) and acetonitrile:formic acid (100:0.1 v/v, solvent B).

2.2. Modification of MWCNTs

Five hundred milligrams of MWCNTs was oxidized with 60 mL H_2SO_4 and HNO_3 (molar ratio = 3:1) at $80 \text{ }^\circ\text{C}$ for 6 h. Then, the obtained mixture was diluted and washed several times with deionized water until the pH value reached 7. The carboxylic-acid-functionalized MWCNT product was obtained by centrifugation, followed by vacuum drying at $60 \text{ }^\circ\text{C}$. Subsequently, 400 mg of this product was dispersed in 60 mL SOCl_2 , and 1 mL DMF was added dropwise. The mixture was stirred for 24 h at $60 \text{ }^\circ\text{C}$, then the residual SOCl_2 was removed by reduced pressure distillation at $20 \text{ }^\circ\text{C}$, as well as by reaction with NaOH solution. Thereafter, 200 mg of the obtained MWCNTs-COCl was mixed with 30 mL THF by ultra-sonication for 30 min [20], followed by the dropwise addition of allylamine solution in DMF (20 mL allylamine dissolved in 10 mL DMF). The mixture was continuously stirred at $60 \text{ }^\circ\text{C}$ for 24 h, and the resulting product (MWCNTs-CH=CH₂) was finally collected by centrifugation.

2.3. Synthesis of the MWCNTs-MIP-template adduct

The MWCNTs-MIP material was prepared by precipitation polymerization, as per the method detailed below. First, 0.1 mmol of the CAPs template were dispersed in 20 mL trichloromethane and acetonitrile (1:3 v/v), along with 0.4 mmol of the 4-VP monomer and 60 mg of MWCNTs-CH=CH₂. Afterwards, EGDMA (2.0 mmol) and AIBN (60 mg) were added, and the mixture was homogenized by sonication for 10 min [21]. Before polymerization, the solution was degassed using a flow of high purity nitrogen. Finally, the polymerization reaction was carried out in a $60 \text{ }^\circ\text{C}$ oil bath for 24 h. The polymeric particulates were separated from the mixture by centrifugation then washed with methanol/acetic acid

(9:1 v/v) using a Soxhlet apparatus until no template was detected by HPLC. Subsequently, the particulates were dried under vacuum at 60 °C to obtain the final solid product. The non-imprinted polymers (MWCNT-NIP) were prepared using the same procedure, but in the absence of the template. the polymerization reaction was carried out in a 60 °C oil bath for 24 h.

2.4. Fabrication of the sensor

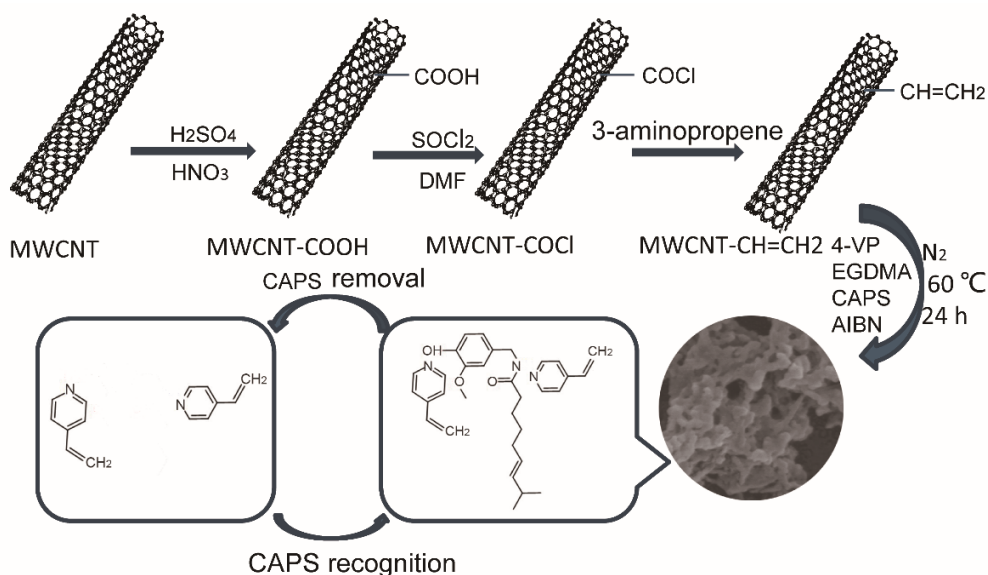
Two milligrams of MWCNT-MIP was dispersed in 1 mL chitosan solution (1%) by ultrasonication for 1 h. Before modification, GCE was polished using 1.0 and 0.05 μm alumina slurry, then it was rinsed thoroughly with ultrapure water. Afterwards, 5 μL of MWCNTs-MIP was dropped on the surface of the pretreated GCE electrode and dried at room temperature. The MWCNTs-NIP and MWCNTs-MIP modified GCE electrodes were prepared in the same way. The modified electrodes were immersed in an HOAc/ethanol mixture (9:1 v/v) for 10 min to extract the template.

2.5. Real sample analysis

Gutter oil samples were supplied by Chongqing Public Security Bureau. Five grams of each sample were transferred to a 10 mL polypropylene-capped centrifuge tube containing 5 mL methanol. The mixture was vortexed for 10 min and centrifuged at 2000 rpm and 4 °C for another 10 min. The upper layer was transferred and filtered through an organic membrane (0.45 μm)[3], and then it was stored at 4 °C for subsequent electrochemical analysis.

3. RESULTS AND DISCUSSION

3.1. Preparation and characterization of MIP



Scheme 1. Schematic representation of the MWCNT-MIP preparation procedure.

As shown in Scheme 1, MWCNTs-MIP synthesis is initiated by reacting 3-aminopropene-modified MWCNTs with CAPS and the 4-vinyl pyridine monomer to form a self-assembly complex that is maintained by hydrogen bonding between the N-H proton of 4-VP and CAPS [21]. This complex is fixed on the surface of MWCNTs by free radical crosslinking reaction between EGDMA and the vinyl-group-functionalized MWCNTs. Finally, the templates in the imprinted polymer are removed in order to expose the special recognition site.

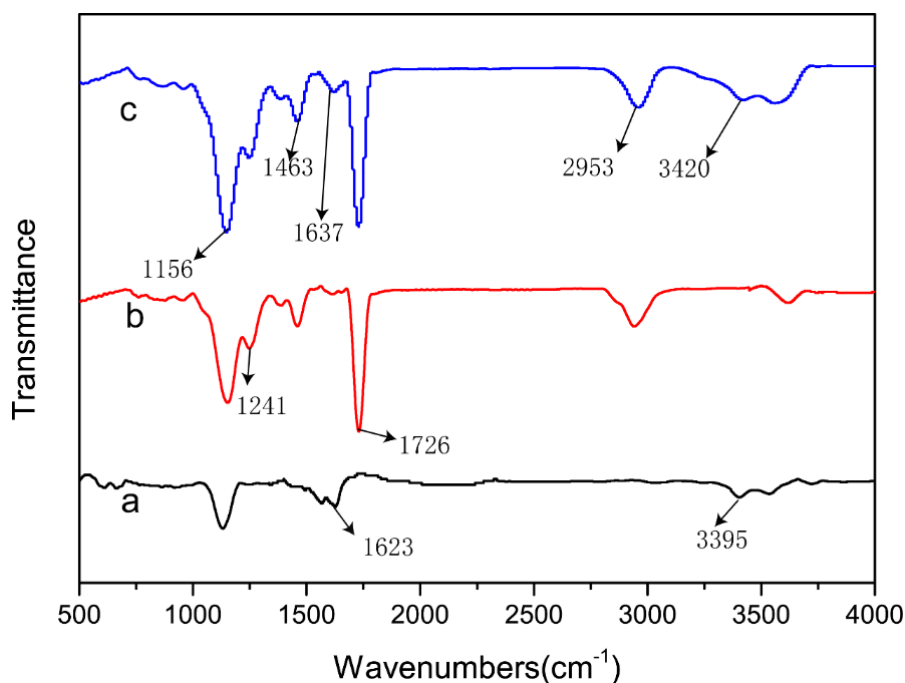


Figure 1. FTIR spectra of (a) MWCNT-CH=CH₂, (b) MWCNT-NIP, and (c) MWCNT-MIP.

The FTIR spectra of the MWCNTs-CH=CH₂, MWCNTs-MIP, and MWCNTs-NIP are shown in Fig. 1. The absorption peaks observed at 1623 and 3395 cm⁻¹ (C=C and N-H stretching vibrations, respectively) in Fig. 1a indicate that the MWCNTs-CH=CH₂ intermediate had been successfully formed [20]. Meanwhile, the MWCNTs-MIP and MWCNTs-NIP spectra (Figs. 1b and 1c) present peaks at 1637 and 1463 cm⁻¹ corresponding to the C=C and C=N stretching vibrations of the 4-vinyl pyridine monomer, respectively. The peaks at 1726 and 1156 cm⁻¹ are characteristic of the C=O and C-O stretching vibrations of EGDMA. The observation of the N-H stretching band at 3200–3500 cm⁻¹ confirms the presence of hydrogen bonds, which in turn proves that the polymer had been successfully synthesized [22-24].

Based on SEM analysis, the lengths and diameters of MWCNTs are in the order of several micrometers and 5–10 nm, respectively (Figs. 2A and 2B). After polymerization, some granular substances are clearly observed on the MWCNT surface. These substances correspond to carbon nanotubes that are embedded in the polymer matrix to form a three-dimensional electroconductive network.

3.2. Voltammetric behavior of CAPS

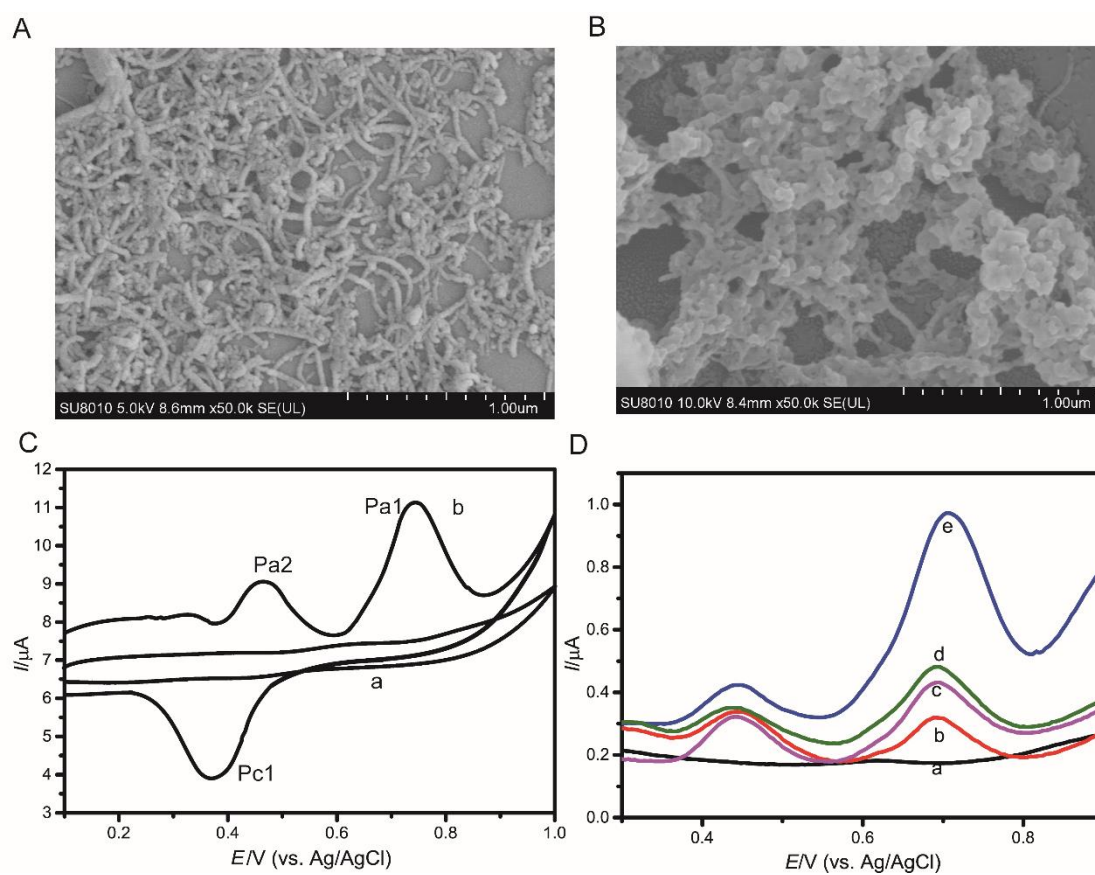


Figure 2. SEM images of (A) MWCNT and (B) MWCNT-MIP (C) Cyclic voltammograms of GCE and MWCNTs-MIP/GCE in 10 μM CAPS solution (pH = 2.0, scan rate = 100 mV/s). D) DPVs of (a) bare GCE, (b) NIP/GCE, (c) MIP/GCE, (d) MWCNT-NIP/GCE, and (e) MWCNT-MIP/GCE in 10 mL 5.0 μM CAPS solution (pH = 2.0).

Figure 2C presents the electrochemical behavior of CAPS at the MWCNTs-MIP-modified GCE and blank GCE in B-R buffer solution. An anodic peak at 0.74 V and a pair of redox peaks at 0.36 and 0.42 V are observed, which is consistent with previous reports [16,17]. Considering that the Pa1 peak shows the highest sensitivity, it was selected as the test index in the following experiments.

To confirm the electrochemical characteristics of MWCNTs-MIP/GCE, the behaviors of CAPS at different modified electrodes, as well as at the bare electrode, were observed by differential pulse voltammetry (DPV) in the potential range of 0.2–0.8 V (vs. Ag/AgCl). The results illustrated in Fig. 2D show great differences in the DPV curves of bare GCE (a), NIP/GCE (b), MIP/GCE (c), MWCNTs-NIP/GCE (d), and MWCNTs-MIP/GCE (e). The oxidation peak current can hardly be observed at the bare glassy carbon electrode, within the investigated potential range. This suggests that this electrode cannot be used to analyze trace levels of CAPS. Meanwhile, the NIP- (curve b) and MIP-modified GCE (curve c) DPV curves exhibit remarkably increased oxidation peak currents, compared to bare GCE, which indicates that both, NIP and MIP exhibit adsorption behavior [25]. The stronger Pa1 signal at MIP/GCE (curve c), compared to the NIP/GCE signal (curve b), indicates that the prepared polymer can provide selective binding sites on the electrode surface [26]. When NIP is bonded to the surface of a

multi-walled carbon nanotube, the response of the modified electrode to CAPS increases appreciably, compared to NIP/GCE (curves b and d in Fig. 2D). The peak current of MWCNTs-MIP/GCE (curve e) is higher than that MWCNTs-NIP/GCE (curve d), indicating that the performance of the latter electrode is better. This is probably due to the excellent conductivity and high surface-to-volume ratio of carbon nanotubes [19].

3.3. Optimization of polymerization

The imprint sites in the imprinted nanomaterial are determined based on the ratio of templates (CAPS) to functional monomers (4-VP) [27]. This ratio was varied in the range of 1:2–1:8 for a template/cross-linker molar ratio of 1:20. Between 1:2 and 1:4, the response currents increase significantly; however, between 1:4 and 1:8, they drop (Fig. 3A).

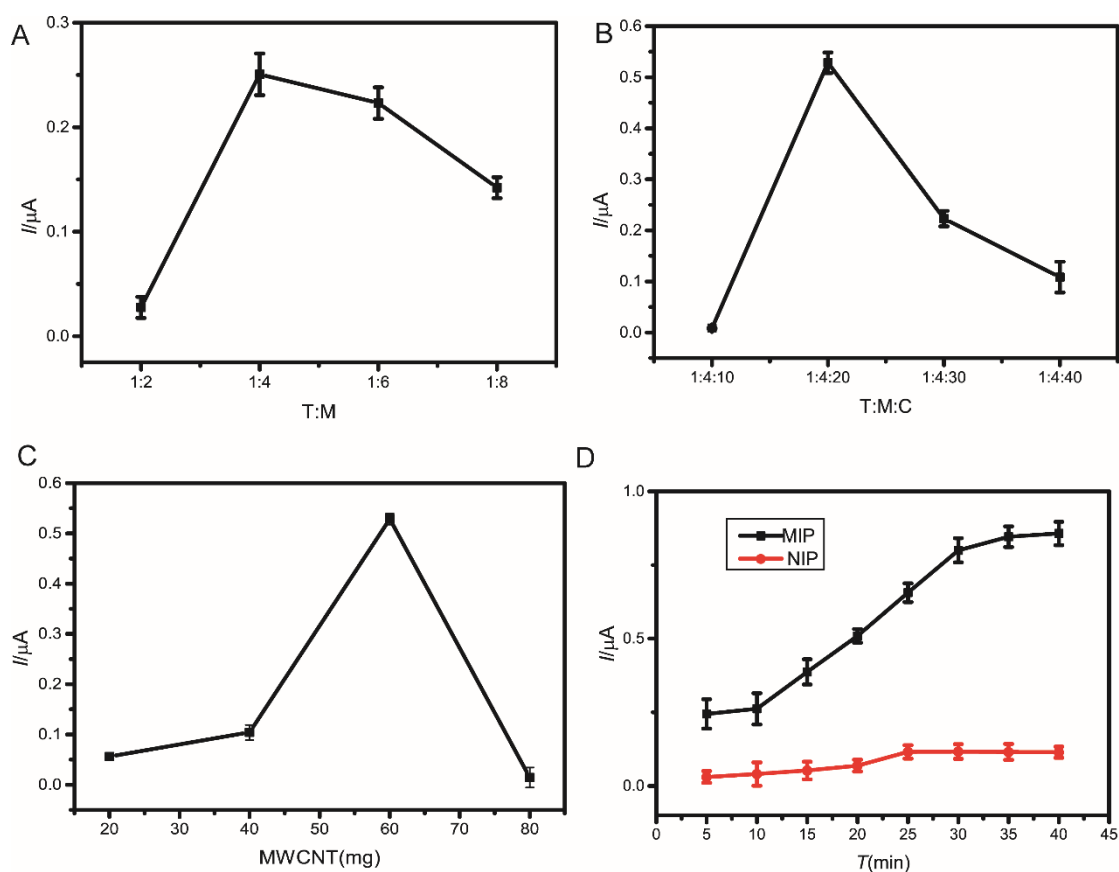


Figure 3. Optimization of the (A) T/M and (B) T/M/C ratios. Effects of (C) incubation time and (D) MWCNT content on DPV response.

This indicates that the optimal of template to monomer ratio is 1:4. As shown in Fig. 3B, the ratio of template (T) /functional monomers (M) / cross-linkers (C) also affects the response current of the proposed sensor [28]. The current rapidly increases with increasing EGDMA between 10 and 20 mg due to the increased number of template-monomer complexes on the MWCNTs. However, excessive crosslinking polymerization of 4-VP by EGDMA in the range of 20–30 mg leads to many recognition

cavities buried in the polymeric network, which ultimately decreases the current response. Therefore, the optimal template/ monomer/cross-linker ratio is 1:4:20.

3.4. Optimization of the electrochemical conditions

The effect of pH on the electrochemical response of $10 \mu\text{mol L}^{-1}$ CAPS in 0.1 M B-R buffer solution at the MWCNTs-MIP-modified electrode was investigated in the range of 2.0–10.0. Fig. 4A shows that the oxidation peak current decreases continuously with increasing pH value, which suggest that acidic conditions favor the binding of CAPS to MIP. The oxidation potential also decreases linearly with increasing pH, as demonstrated in Fig. 4B. The equation of the linear relation between E_{pa1} and pH is $E_{pa1}(\text{mV}) = -0.0615\text{pH} + 0.80$, and the corresponding correlation coefficient (R^2) is 0.99. The mechanism of the electrochemical redox reaction of CAPS is presented in Fig. S1 [32-35].

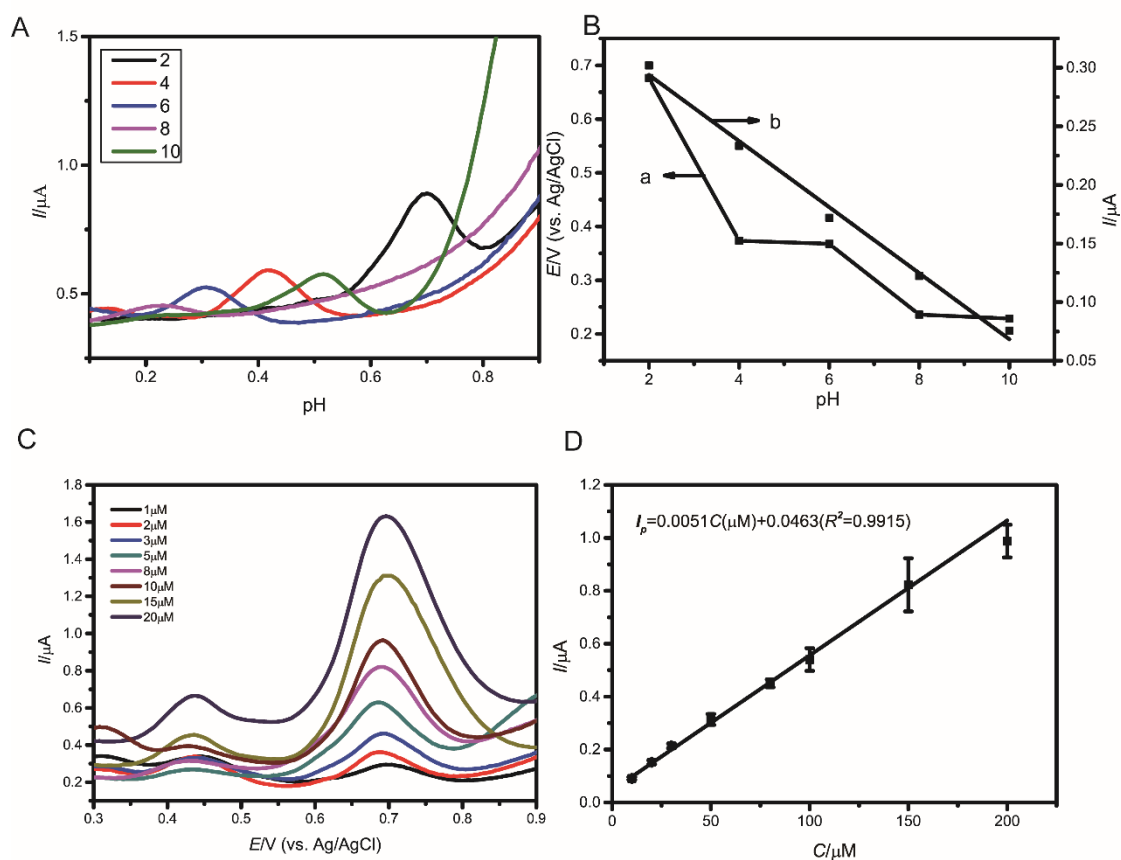


Figure 4. Effect of pH on (a) MWCNT-MIP/GCE DPVs and (b) peak potential and current in $5.0 \mu\text{M}$ CAPS. (c, d) DPV responses of the MWCNT-MIP-modified electrode in B-R buffer solution containing different concentrations of CAPS.

The effect of incubation time is explored at $\text{pH} = 2.0$, as shown in Fig. 3D. The obtained results indicate that the peak current increases with increasing incubation time between 5 and 30 min. However,

the rate of current increase at the MWCNTs-NIP-modified electrode is substantially less than that at MWCNTs-MIP. The currents of MWCNTs-MIP and MWCNTs-NIP GCEs become nearly constant beyond 30 min of incubation, which means that 30 min is the optimal incubation time.

Film thickness and MWCNT amount are important factors affecting sensor performance. Sensors prepared with 5.0 μL of the polymer solution yield optimal electrochemical behavior. In the range of 20–60 mg, the current response gradually increases with increasing MWCNT amount (Fig. 3C) due to the availability of larger surface areas for MIP loading. Beyond 60 mg, the current decreases due to reduced effective recognition sites on the MWCNT surface.

3.5. Performance of the sensor

The DPV response of the MWCNTs-MIP-modified electrode was investigated for various concentrations of CAPS (1.0–20 μM), under optimum conditions (Fig. 4C). The curve presented in Fig. 4D shows good linearity between oxidation peak current (I_p , μA) and concentration (C , $\mu\text{mol L}^{-1}$), with $R^2 = 0.9915$ and $I_p(\mu\text{A}) = 0.0051C(\mu\text{mol L}^{-1}) + 0.0463$. Using $C_m = 3S_d/S$ (S is the slope of the calibration curve in the linear range and S_d is the standard deviation of the blank response based on five replicate measurements in B-R buffer solution), the limit of detection was found to be 0.02 μM . Compared to other reported capsaicin sensors, the sensor developed herein exhibits excellent electrocatalytic performance with good linearity and selectivity in the investigated capsaicin concentration range (Table 1).

Table 1. Comparison of the different sensors for the detection of CAPS.

Detection method	Modified electrode	Detection limit	linear range (μM)	References
AdsSV/CV	CNTs / GCE	0.31 $\mu\text{mol L}^{-1}$	0.5-60	[15]
AdsSV	Boron-Doped Diamond Electrode	0.034 $\mu\text{mol L}^{-1}$	0.16-20	[29]
LSV/SWV/DPV/Amperometry	MCFs/CPE	0.08 $\mu\text{mol L}^{-1}$	0.76-11.65	[30]
UV-Visible	MBTH/Sol-gel/Butyl acrylate/HRP/Chitosan	0.17 mM	0.2–4.0 mM	[31]
EIS-CV	MWCNT-SPE	0.45 $\mu\text{mol L}^{-1}$	-	[32]
SPME-GC-MS	-	0.045 $\mu\text{mol L}^{-1}$	0.357-0.433	[33]
CE	-	2.16 $\mu\text{mol L}^{-1}$	3.28-1311	[34]
DPV/CV/EIS	MnSeNPs /GCE	0.05 $\mu\text{mol L}^{-1}$	-	[35]
DPV	NH ₂ -FMS/CPE	0.02 $\mu\text{mol L}^{-1}$	0.04-4	[16]

DPV/CV	PAL/Nafion/MWCNTs/Pt-E	0.61 $\mu\text{mol L}^{-1}$	-	[17]
HPLC	-	0.09 $\mu\text{g /g}$	-	[36]
AdSV/ DPV	SPCE	0.05 $\mu\text{mol L}^{-1}$	0.16-16.37	[37]
DPSV	PSS-Grp/SPE	0.1 $\mu\text{mol L}^{-1}$	0.3-70	[38]
SWV/CV	PPy-Bi ₂ O ₃ -GO/GCE	0.059 $\mu\text{mol L}^{-1}$	0.26-2.62	[39]
DPV	MWCNTs-MIP	0.02 $\mu\text{mol L}^{-1}$	0.05-100	Present work

3.6. Comparison of different capsaicin sensors

Table 1 compares different methods reported in the literature for the detection of capsaicin. According to the listed data, electrochemical methods allow for rapid, miniaturized, and on-the-spot detection of the analyte, even in trace amounts, unlike other methods based on large instruments. In addition, some of the traditionally used enzyme-based biosensors are affected by temperature, pH, and humidity, and they cannot be easily prepared. Comparatively, electrochemical sensors modified with molecularly imprinted polymers are more stable and selective. In summary, the proposed sensor is characterized by the favorable properties of low detection limit, wide detection range, and specific recognition.

3.7. Selectivity

To evaluate the selectivity of the MWCNTs-MIP/GCE sensor, the detection efficiency of CAPS structural analogues including 6-gingerol, dihydrocapsaicin, and catechol was tested under optimum conditions, at the same concentration as CAPS.

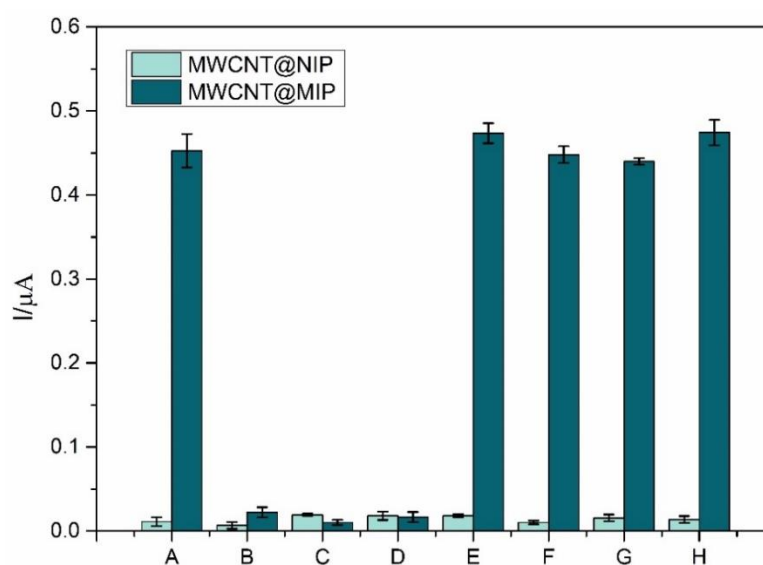


Figure 5. DPV responses in (A) CAPS, (B) dihydrocapsaicin, (C) 6-gingerol, (D) catechol, (E) Cu²⁺, (F) Mg²⁺, (G) Na⁺, and (H) K⁺ solutions.

As shown in Fig. 5, both, MIP- and NIP-modified electrodes have little response towards the tested interferents. Moreover, the peak current of CAPS is not affected by the presence of interfering ions in gutter oils (ex. Cu^{2+} , Mg^{2+} , Na^+ , and K^+), even at concentrations 50 times greater than that of CAPS. This indicated that the MWCNTs-MIP prepared herein is highly selective in capsaicin detection.

3.8. Repeatability, stability, and reproducibility of the electrode

The repeatability of the sensor was explored based on the 10-time-repeated detection of $10 \mu\text{mol L}^{-1}$ CAPS in B-R ($\text{pH} = 2.0$). The relative standard deviation (RSD) of the repeated measurements was found to be 4.9%, which suggests that the prepared sensor exhibits good repeatability. The reproducibility of the electrode was also estimated by repetitive measurements in $10 \mu\text{mol L}^{-1}$ capsaicin solution. The obtained results show a relative standard deviation (RSD) of 3.58% ($n = 8$). As for stability, it was examined by measuring the response in $10 \mu\text{mol L}^{-1}$ CAPS after one month of storing the electrochemical sensor in air at room temperature. The RSD value of 4.3% ($n = 6$) indicates that the electrode is highly stable.

3.9. Real sample analysis

In order to evaluate the capsaicin detection efficiency of MWCNTs-MIP-modified electrodes in real samples, gutter oil was analyzed using the proposed sensor, after 150 times dilution with B-R buffer. The results demonstrate that the MWCNTs-MIP sensor possesses excellent accuracy in terms of RSD values (Table 2).

Table 2. Determination of capsaicin in extract of gutter oils by MWCNT-MIP/GCE($n=6$).

Sample	Origin value/ μM	Spiked/ μM	found/ μM	Recovery (%)	RSD (%)
1	4.4	5.0	9.3	98.9	1.7
2	5.3	5.0	10.5	101.9	2.5
3	4.2	5.0	8.9	96.7	3.8

Moreover, the recovery values vary between 96.7 and 101.9%, indicating that the fabricated electrochemical biosensor is as efficient as an HPLC analyzer in detecting CAPS. Therefore, it can be used to analyze this compound in gutter oils.

4. CONCLUSION

A novel electrochemical sensor was prepared for the identification and quantification of capsaicin (CAPS) in gutter oil samples. This sensor is composed of MWCNTs modified with molecularly

imprinted polymeric film, and it is capable of selectively recognizing and sensitively detecting CAPS. Moreover, it exhibits a wide linear range of detection, a relatively low detection limit ($0.02 \mu\text{mol L}^{-1}$), good recovery (96.7–101.9%), and high stability and repeatability. Therefore, the MWCNTs-MIP-based sensor may be applied in the detection of CAPS in gutter oil samples.

CONFLICT OF INTEREST

The authors declare that they do not have any commercial or associative interests that represent a conflict of interest in connection with the work submitted.

ACKNOWLEDGEMENTS

This research was supported by the institute of Forensic Medicine, Chongqing Medical University, China.

References

1. T. T. Ng, P. K. So, B. ZhengZ. P. Yao, *Anal Chim Acta*, 884 (2015) 70.
2. J. Li, N. CuiJ. Liu, *Glob Health Promot*, 24 (2017) 75.
3. F. Ma, Q. Yang, B. Matthaus, P. Li, Q. ZhangL. Zhang, *J Chromatogr B Analyt Technol Biomed Life Sci*, 1021 (2016) 137.
4. H.-G. Janssen, H. Steenbergens. de Koning, *Eur. J. Lipid Sci. Technol*, 111 (2009) 1171.
5. A. Gliszczynska-SwigloE. Sikorska, *J Chromatogr A*, 1048 (2004) 195.
6. M. Chen, X. Hu, Z. Tai, H. Qin, H. Tang, M. LiuY. Yang, *Food Anal. Meth.*, 6 (2012) 28.
7. P. L. Buldini, D. FerriJ. L. Sharma, *J. Chromatogr. A*, 789 (1997) 549.
8. R. AparicioR. Aparicio-Ruiz, *J Chromatogr A*, 881 (2000) 93.
9. M. Amzad HossainS. M. Salehuddin, *Arabian Journal of Chemistry*, 5 (2012) 391.
10. M. D. GuillénP. S. Uriarte, *Food Control*, 28 (2012) 59.
11. M. D. GuillénA. Ruiz, *Eur. J. Lipid Sci. Technol.*, 110 (2008) 52.
12. M. D. GuillénA. Ruiz, *Food Chem.*, 96 (2006) 665.
13. F. LuX. Wu, *Food Control*, 41 (2014) 134.
14. S. Alexander, P. Baraneedharan, S. Balasubrahmanyans. Ramaprabhu, *Mater Sci Eng C Mater Biol Appl*, 78 (2017) 124.
15. R. T. Kachoosangi, G. G. WildgooseR. G. Compton, *Analyst*, 133 (2008) 888.
16. Y. Ya, L. Mo, T. Wang, Y. Fan, J. Liao, Z. Chen, K. S. Manoj, F. Fang, C. LiJ. Liang, *Colloids Surf B Biointerfaces*, 95 (2012) 90.
17. M. I. Sabela, T. Mpanza, S. Kanchi, D. SharmaK. Bisetty, *Biosens Bioelectron*, 83 (2016) 45-53.
18. A. Pathak, S. ParveenB. D. Gupta, *Nanotechnology*, 28 (2017) 355503.
19. H. Ding, R. Chen, M. Liu, R. Huang, Y. Du, C. Huang, X. Yu, X. FengF. Liu, *RSC Advances*, 6 (2016) 43526.
20. B. B. Prasad, R. Madhuri, M. P. TiwariP. S. Sharma, *Electrochim. Acta*, 55 (2010) 9146.
21. X. Ma, W. Ji, L. Chen, X. Wang, J. LiuX. Wang, *J Sep Sci*, 38 (2015) 100.
22. L. Cheng, S. Pan, C. Ding, J. HeC. Wang, *J Chromatogr A*, 1511 (2017) 85.
23. N. Chen, L. Chen, Y. Cheng, K. Zhao, X. WuY. Xian, *Talanta*, 132 (2015) 155.
24. L. Chen, H. T. Lian, X. Y. SunB. Liu, *Anal Biochem*, 526 (2017) 58.
25. T. Alizadeh, F. Atashi, M. R. Ganjali, *Talanta*, 194 (2019) 415.
26. A. R. Bagheri, M. Arabi, M. Ghaedi, A. Ostovan, X. Wang, J. Li, L. Chen, *Talanta*. 195 (2019) 390.
27. J. Pan, W. Chen, Y. Ma, G. Pan, *Chem. Soc. Rev.* 47 (2018) 5574.
28. O. S. Ahmad, T. S. Bedwell, C. Esen, A. Garcia-Cruz, S. A. Piletsky, *Trends Biotechnol*, 37 (2019)

- 294.
29. Y. Yardim, *Electroanalysis*, 23 (2011) 2491.
 30. Z. Xue, C. Hu, H. Rao, X. Wang, X. Zhou, X. Liu, X. Lu, *Anal. Methods*, 7 (2015) 1167.
 31. M. A. Rosmawani Mohammad, Lee Yook Heng, *Sens. Actuator B-Chem*, 190 (2014) 593.
 32. P. Randviir, J. P. Metters, J. Stainton, C. E. Banks, *Analyst*, 138 (2013) 2970.
 33. E. R.-M. Araceli Peña-Alvarez, L. A. Alvarado-Suárez., *Journal of Chromatography A*, 1216 (2009) 2843.
 34. L. Liu, X. Chen, J. Liu, X. Deng, W. Duan, S. Tan, *Food Chem*, 119 (2010) 1228.
 35. R. Sukanya, M. Sakthivel, S. M. Chen, T. W. Chen, F. M. A. Al-Hemaid, M. Ajmal Ali, M. S. Elshikh, *Mikrochim Acta*, 185 (2018) 313.
 36. Z. A. A. Othman, Y. B. H. Ahmed, M. A. Habila, A. A. Ghafar, *Molecules*, 16 (2011) 8919.
 37. W. Lyu, X. Zhang, Z. Zhang, X. Chen, Y. Zhou, H. Chen, H. Wang, M. Ding, *Sens. Actuator B-Chem*, 288 (2019) 65.
 38. Y. Wang, B.-B. Huang, W.-L. Dai, B. Xu, T.-L. Wu, J.-P. Ye, J.-S. Ye, *Anal. Sci.* 33 (2017) 793.
 39. A. Verma, R. Jain, *J. Electrochem. Soc*, 164 (2017) H908.

© 2020 The Authors. Published by ESG (www.electrochemsci.org). This article is an open access article distributed under the terms and conditions of the Creative Commons Attribution license (<http://creativecommons.org/licenses/by/4.0/>).